Available online at www.sciencedirect.com
SCIENCE DIRECT®
Chemistry and Physics of Lipids 141 (2006) 48–65
CPL
CHEMISTRY AND PHYSICS OF LIPIDS
www.elsevier.com/locate/chemphyslip

Review

Lipid conformation in crystalline bilayers and in crystals of transmembrane proteins

Derek Marsh [a,*], Tibor Páli [b]

[a] *Max-Planck-Institut für biophysikalische Chemie, Abteilung Spektroskopie, 37070 Göttingen, Germany*
[b] *Institute of Biophysics, Biological Research Centre, 6701 Szeged, Hungary*

Received 17 November 2005; accepted 20 February 2006
Available online 15 March 2006

Abstract

Dihedral torsion angles evaluated for the phospholipid molecules resolved in the X-ray structures of transmembrane proteins in crystals are compared with those of phospholipids in bilayer crystals, and with the phospholipid conformations in fluid membranes. Conformations of the lipid glycerol backbone in protein crystals are not restricted to the *gauche* C1–C2 rotamers found invariably in phospholipid bilayer crystals. Lipid headgroup conformations in protein crystals also do not conform solely to the bent-down conformation, with *gauche–gauche* configuration of the phospho-diester, that is characteristic of phospholipid bilayer membranes. This suggests that the lipids that are resolved in crystals of membrane proteins are not representative of the entire lipid–protein interface. Much of the chain configurational disorder of the membrane-bound lipids in crystals arises from energetically disallowed *skew* conformations. This indicates a configurational heterogeneity in the lipids at a single binding site: eclipsed conformations occur also in some glycerol backbone torsion angles and C–C torsion angles in the lipid headgroups. Stereochemical violations in the protein-bound lipids are evidenced by one-third of the ester carboxyl groups in non-planar configurations, and certain of the carboxyls in the *cis* configuration. Some of the lipid structures in protein crystals have the incorrect enantiomeric configuration of the glycerol backbone, and many of the branched methyl groups in structures of the phytanyl chains associated with bacteriorhodopsin crystals are in the incorrect *S*-configuration.

Keywords: Lipid–protein interactions; Headgroup conformation; Chain conformation; Torsion angles

Contents

* Corresponding author. Tel.: +49 551 201 1285; fax: +49 551 201 1501.
E-mail address: dmarsh@gwdg.de (D. Marsh).

0009-3084/$ – see front matter © 2006 Elsevier Ireland Ltd. All rights reserved.
doi:10.1016/j.chemphyslip.2006.02.005

1. Introduction

A considerable and steadily growing number of endogenous lipids have now been resolved in the high-resolution X-ray structures of integral membrane proteins (for reviews see Fyfe et al., 2001; Pebay-Peyroula and Rosenbusch, 2001; Lee, 2003). Amongst these are phosphatidylcholine in association with cytochrome *c* oxidase from *Paracoccus denitrificans* (Iwata et al., 1995; Harrenga and Michel, 1999), cardiolipin and phosphatidylethanolamine associated with various bacterial photosynthetic reaction centres (McAuley et al., 1999; Fyfe et al., 2000; Nogi et al., 2000), and a variety of diphytanyl lipid moieties in association with bacteriorhodopsin (Essen et al., 1998; Luecke et al., 1999; Belrhali et al., 1999; Takeda et al., 2000). Phosphatidylethanolamine, phosphatidylcholine, phosphatidylglycerol and cardiolipin moieties have also been reported in association with bovine cytochrome *c* oxidase (Tsukihara et al., 1996; Mizushima et al., 1999). More recently, phosphatidylglycerol and galactosyl diacylglycerol have been resolved in association with photosystem I of a cyanobacterium (Jordan et al., 2001), and with a plant light-harvesting complex (Liu et al., 2004). The transmembrane domains of all the aforementioned proteins are α-helical. In addition, a molecule of lipopolysaccharide has been resolved in association with the β-barrel outer-membrane protein FhuA (Ferguson et al., 2000).

From the point of view of lipid–protein interactions, it is of direct interest to compare the above data with the structural information available from lipid bilayers. The X-ray structures of phospholipids in bilayer crystals provide a wealth of detail on the conformations and stereochemistry of phospholipids when close-packed in membranes (Hauser et al., 1981; Pascher et al., 1992; Pascher, 1996). A detailed comparison with this lipid data will therefore delineate the perturbation of the molecular configuration by the protein–lipid interaction.

Here, we review analyses of the torsion angles of lipid molecules in crystals of transmembrane proteins and of the corresponding lipids in bilayer single crystals. Comparison of the two reveals stereochemical violations and possible conformational hetereogeneity in the structures of the lipids associated with crystalline transmembrane proteins.

2. Definition of lipid torsion angles

Fig. 1a gives the notation for the torsion angles in a diacyl lipid, and explicit definitions are given in Table 1 (Sundaralingam, 1972). This notation is commonly used for describing the crystal conformations of glycerolipids and sphingolipids (Hauser et al., 1981; Pascher et al., 1992), except that the numbering of the glycerol backbone C-atoms is reversed to conform with the *sn*-convention (IUPAC-IUB Commission on Biochemical Nomenclature (CBN), 1977) for eucaryotic and bacterial glycerolipids. Fig. 1b gives the classification of the staggered and eclipsed rotamers used for conformational description of lipids, according to the range of torsion angle (Klyne and Prelog, 1960). Equiv-

Table 1
Definition of torsion angles with atom numbering of Fig. 1

θ_1	C(1)–C(2)–C(3)–O(31)
θ_2	O(21)–C(2)–C(3)–O(31)
θ_3	O(11)–C(1)–C(2)–C(3)
θ_4	O(11)–C(1)–C(2)–O(21)
α_1	C(2)–C(3)–O(31)–P
α_2	C(3)–O(31)–P–O(32)
α_3	O(31)–P–O(32)–C(31)
α_4	P–O(32)–C(31)–C(32)
α_5	O(32)–C(31)–C(32)–N
β_1	C(3)–C(2)–O(21)–C(21)
β_2	C(2)–O(21)–C(21)–C(22)
β_3	O(21)–C(21)–C(22)–C(23)
β_4	C(21)–C(22)–C(23)–C(24)
γ_1	C(2)–C(1)–O(11)–C(11)
γ_2	C(1)–O(11)–C(11)–C(12)
γ_3	O(11)–C(11)–C(12)–C(13)
γ_4	C(11)–C(12)–C(13)–C(14)

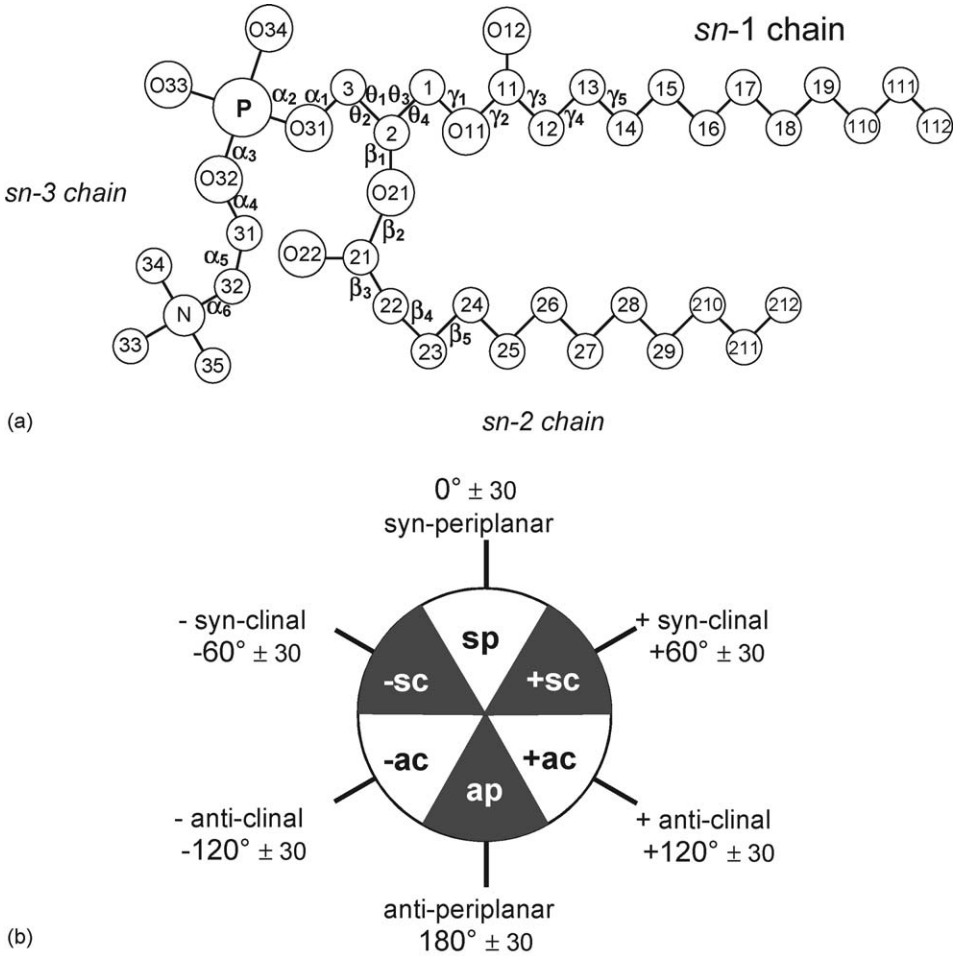

Fig. 1. (a) Notation for torsion angles in a diacyl glycerolipid (Sundaralingam, 1972). The chain designation is that for the *sn*-3 phosphatidyl enantiomer. (b) Designation of torsion-angle ranges for staggered and eclipsed rotamers (Klyne and Prelog, 1960).

alent conformational designations frequently used are: *trans*, t (ap); *gauche*, g (sc); *skew*, s (ac); and *cis*, c (sp).

3. Lipid bilayers

3.1. Glycerol backbone configuration in bilayer crystals

The backbone conformation in crystals of glycerolipids has been studied by Pascher et al. (1992): it is characterised relative to the lipid chains by the θ_4 and θ_2 torsion angles. The torsion angle about the glycerol C(1)–C(2) bond, viz., θ_4, specifies the relative orientation of the *sn*-1/*sn*-3 and *sn*-2 chains, and that about the C(2)–C(3) bond, viz., θ_2, defines the orientation of the headgroup relative to the *sn*-2 chain. In addition, the corresponding chain stacking is characterised by which of the two chains is the leading or straight-extending chain. This is designated by γ for a leading *sn*-1 chain and by β for a leading *sn*-2 chain. The chain backbone configuration in crystals is specified by the Pascher notation as: θ_4/leading chain/θ_2 (Pascher et al., 1992). That of the glycerol moiety itself is described by the corresponding θ_3/θ_1 combination of torsion angles. In the sc/γ configuration, the glycerol backbone is oriented approximately parallel, and in the sc/β configuration almost perpendicular, to the bilayer normal. In both the $-$sc/γ and $-$sc/β configurations, however, the backbone of the glycerol moiety is oriented at approximately 45° to the bilayer normal.

The torsion angles of the glycerol backbone in lipid crystals correspond exclusively to staggered conformations (Pascher et al., 1992). In principle, all combinations of θ_4/θ_2 staggered torsion angles are represented in lipid crystal structures, but only those with $\theta_4 = +$sc or $-$sc allow the parallel chain stacking charac-

Table 2
Torsion angles (°) of crystalline phospholipids, classified according to θ_4/leading chain/θ_2 and glycerol configuration θ_3/θ_1[a]. Structures of phospholipids in fluid bilayers (L_α) derived from NMR are included for comparison

Lipid[b]	α_1	α_2	α_3	α_4	α_5	θ_1	θ_2	θ_3	θ_4	β_1	β_2	β_3	β_4	γ_1	γ_2	γ_3	γ_4	Ref.[c]
sc/γ/sc, $\theta_3/\theta_1 = tg^-$ (27% of crystal structures)																		
DLPE	−154	58	66	106	67	−52	65	−172	69	97	179	−119	65	−178	173	179	−171	1
sc/γ/−sc, θ_3/θ_1 = tt (30% of crystal structures)																		
DMPC B	177	−74	−47	−150	54	168	−80	166	51	120	179	−134	67	102	176	180	180	2,3
sc/γ/ap, $\theta_3/\theta_1 = tg^+$ (3% of crystal structures)																		
DMPC A	163	62	68	143	−64	58	177	−178	63	82	172	−81	45	−177	168	−173	178	2,3
sc/β/sc, $\theta_3/\theta_1 = tg^-$ (9% of crystal structures)																		
DMPA	153					−54	62	−179	62	87	172	164	179	−142	180	−119	73	4
sc/β/ap, $\theta_3/\theta_1 = tg^+$ (3% of crystal structures)																		
DLPA	−151					64	−171	−172	62	83	174	164	173	−173	−176	−77	70	2
−sc/γ/−sc, $\theta_3/\theta_1 = g^+t$ (15% of crystal structures)																		
$DLPEM_2$	179	65	54	144	−96	176	−66	56	−60	148	173	−57	176	129	−167	166	175	5
−sc/γ/ap, $\theta_3/\theta_1 = g^+g^+$ (9% of crystal structures)																		
DMPG B	116	58	78	−147	−173	71	179	45	−58	157	180	−50	−175	122	179	142	174	6
−sc/β/−sc, $\theta_3/\theta_1 = g^+t$ (3% of crystal structures)																		
DMPG A	−146	−76	−86	143	180	151	−78	64	−63	159	178	178	−179	164	−170	110	−57	6
DMPC L_α	110	170	–	–	–	−175	(−55)[d]	−95	(145)[d]	145	110	–	–	−70	180	–	–	7
DPPC L_α[e]	±170	∓60	∓64	∓145	±81													8
DPPE L_α[e]	±193	±50	±64	±96	±87													9

[a] α_i, θ_i, β_i and γ_i are torsion angles of headgroup, glycerol backbone, *sn*-2 chain and *sn*-1 chain, respectively (see Hauser et al., 1981 and Fig. 1).
[b] DLPE, dilauroyl phosphatidylethanolamine; DMPA, dimyristoyl phosphatidic acid; DLPA, dilauroyl phosphatidic acid; $DLPEM_2$, dilauroyl dimethylphosphatidylethanolamine; DMPC A and B, dimyristoyl phosphatidylcholine; DMPG A and B, dimyristoyl phosphatidylglycerol; DMPC L_α, liquid-crystalline state of dimyristoyl phosphatidylcholine bilayers; DPPC L_α, liquid-crystalline state of dipalmitoyl phosphatidylcholine bilayers; DPPE L_α, liquid-crystalline state of dipalmitoyl phosphatidylethanolamine bilayers.
[c] References: 1, Elder et al. (1977); 2, Pascher et al. (1992); 3, Pearson and Pascher (1979); 4, Harlos et al. (1984); 5, Pascher and Sundell (1986); 6, Pascher et al. (1987); 7, Hong et al. (1996); 8, Seelig et al. (1977); 9, Seelig and Gally (1976).
[d] Calculated from θ_1 and θ_3, respectively.
[e] Two interconverting enantiomers.

teristic of a membrane bilayer arrangement. In addition, the ±sc conformations for θ_4 and θ_2 are favoured by the "gauche effect" found in polyoxyethylene (Pascher et al., 1992; Abe and Mark, 1976). Torsion angles for diacyl phospholipids representing the different conformational possibilities in membrane bilayer crystals are given in Table 2. The combinations sc/β/−sc, −sc/γ/sc and −sc/β/sc are not represented because each would rotate the headgroup back into the bilayer, and the latter two also exhibit an energetically unfavourable $\theta_3/\theta_1 = g^+g^-$ glycerol configuration (Pascher et al., 1992). For a similar reason, the θ_4/θ_2 = ap/ap configuration (with $\theta_3/\theta_1 = g^-g^+$) is also strongly disfavoured intramolecularly. The relative occurrences of the different configurations in 33 lipid crystal structures are: sc/γ/sc, 27%; sc/γ/−sc, 30%; sc/γ/ap, 3%; sc/β/sc, 9%; sc/β/ap, 3%; −sc/γ/−sc, 15%; −sc/γ/ap, 9%; −sc/β/−sc, 3% (Pascher et al., 1992). The sc/γ/sc ($\theta_3/\theta_1 \equiv tg^-$) and sc/$\gamma$/−sc ($\theta_3/\theta_1 \equiv$ tt) configurations are therefore particularly strongly represented, and a *trans* (ap) conformation for θ_2 is disfavoured relative to *gauche* (±sc).

Table 2 also lists torsion angles derived from solid state NMR measurements for phosphatidylcholine (DMPC) in fully hydrated fluid bilayer membranes (Hong et al., 1996). This core configuration corresponds to a single structure that is compatible with all 20 anisotropic NMR couplings measured for the backbone region of phosphatidylcholine. The C(1)–C(2) torsion angle in the glycerol backbone ($\theta_3 = -95°$) is midway between staggered and eclipsed. It thus corresponds to a relatively high-energy conformation. Approximately, the backbone configuration can be described as θ_4/θ_2 = ap/−sc ($\theta_3/\theta_1 \equiv g^-t$), although the θ_4 torsion is biased more strongly towards ac. This deviation of θ_4 from a strictly *trans* (ap) conformation, in combination with the unusual γ_1 and β_2 torsion angles, allows parallel chain stacking, but results in a relatively high internal conformational energy. This energy penalty could be removed if, instead of a sin-

gle fixed conformation, it is assumed that the θ_4 torsion angle exchanges rapidly on the NMR timescale, between staggered conformers. High resolution NMR of monogalactosyl diacylglycerol in oriented bicelles has been interpreted in terms of a single predominant sc/γ/−sc configuration (Howard and Prestegard, 1995). On the other hand, high resolution NMR studies of phospholipid micelles were interpreted in terms of a rapid equilibrium between conventional, low-energy rotamers $\theta_4 = +$sc and −sc in an approximately 2:1 ratio (Hauser et al., 1988).

3.2. Headgroup configuration in bilayer crystals

The conformation of the headgroups of phospholipids in bilayer crystals has been reviewed by Pascher et al. (1992). In all cases, the headgroup lies preferentially parallel to the bilayer plane and its internal conformation is strikingly constant. Only the α_4 torsion angle about the O(32)–C(31) bond displays some limited variability. Two mirror image configurations are found in which the signs of the α_2/α_3 torsion angles are reversed, even for non-racemic systems.

For phosphatidylethanolamine and its *N*-methylated derivatives, including phosphatidylcholine, the headgroup configuration in bilayer crystals is specified by: $\alpha_1 =$ ap, $\alpha_2 = \pm$sc, $\alpha_3 = \pm$sc, $\alpha_4 =$ ap to $\pm$ac, and $\alpha_5 = \mp$sc, where the upper and lower signs represent the mirror images (see Table 2). The correlated $\alpha_2/\alpha_3 = \pm$sc/$\pm$sc conformation is that expected on energetic grounds for a phosphate diester (Chandrasekhar et al., 2003). The $\pm$sc/$\pm$sc combination is ca. 1 kcal/mol more favourable than the next lowest lying $\alpha_2/\alpha_3 = \pm$sc/ap combination, even after bond angle optimisation (Gorenstein and Kar, 1977). The C(31)–C(32) torsion angle α_5 is exclusively either −sc or +sc, and its sign is correlated with the size of the α_4 torsion angle. This configuration is determined by internal electrostatic attraction that directs the positively charged nitrogen to the phosphate oxygens. In lipid–protein complexes, interaction of the lipid nitrogen with the protein may be preferred over this internal interaction. In fluid lipid bilayers, the deuterium and phosphorus NMR spectral anisotropies for the polar headgroups of both dipalmitoyl phosphatidylcholine (DPPC) and dipalmitoyl phosphatidylethanolamine (DPPE) can be described by a rapid interconversion between the two mirror-image configurations that are observed in the phospholipid crystals (Seelig et al., 1977; Seelig and Gally, 1976, and see Table 2).

In bilayer crystals of dimyristoyl phosphatidylglycerol, the headgroup configuration of the two optical enantiomers is specified by: $\alpha_1 = \mp$ac, $\alpha_2 = \mp$sc, $\alpha_3 = \mp$sc, $\alpha_4 = \pm$ac, $\alpha_5 =$ ap and $\alpha_6 = \mp$sc (see Table 2). Here, the upper signs correspond to the enantiomer with the natural 1-*sn*-glycerol configuration. The corresponding conformations of the glycerol oxygens are: $\alpha_{5O/O}/\alpha_{6O/O} = \pm$sc/$\pm$sc (Pascher et al., 1992, 1987). This is because $\alpha_5 - \alpha_{5O/O} = +120^\circ$ for the 1-*sn* enantiomer and -120° for the 3-*sn* enantiomer, and vice versa for $\alpha_6 - \alpha_{6O/O}$. The correlated α_2/α_3 conformations in dimyristoyl phosphatidylglycerol are again the $\pm$sc/$\pm$sc combination expected for a phosphate diester. In contrast to the phosphocholine/ethanolamine headgroup, the α_5 torsion angle in phosphatidylglycerol is ap (i.e., *trans*) and it is α_6 that is in the $\mp$sc (i.e., *gauche*) conformation.

3.3. Chain configuration in bilayer membranes

The sp^3-hybridized C–C single bonds in lipid bilayer crystals are restricted mostly to staggered conformations (Pascher et al., 1992). Eclipsed conformations carry an energy penalty that depends on the substituent atoms. For polymethylene chains, the rotational barrier that corresponds to the $\pm$ac eclipsed positions is contributed almost exclusively by the intrinsic threefold rotational potential (Borisova and Vol'kenshtein, 1961; Abe et al., 1966). The dependence of the conformational energy on torsion angles, ϕ, in the *trans* (ap) to *gauche* ($\pm$sc) range may therefore be approximated by (see, e.g., Flory, 1969):

$$E(\phi) \approx E_\sigma + \frac{1}{2}(E_o - E_\sigma)(1 + \cos 3\phi) \quad (1)$$

where $E_o \approx 3$ kcal/mol is the rotational barrier height and E_σ is the energy of the neighbouring potential minimum (see Fig. 2). For the *trans* (ap) potential minimum, $E_\sigma \equiv E_t = 0$, and for the *gauche* ($\pm$sc) minima, $E_\sigma \equiv E_g \approx 0.5$ kcal/mol. Eq. (1) can be used to estimate the conformational energies corresponding to the torsional angle ranges defined in Fig. 1b. The energy span over the 0–30° range about the *trans* conformation is E(ap) ≈ 0–1.5 kcal/mol, that for the *gauche* conformation is $E(\pm\text{sc}) \approx 0.5$–1.75 kcal/mol, and that for the $\pm$ac eclipsed conformation is $E(\pm\text{ac}) \approx 1.5$–3 kcal/mol. The extremes assigned to the staggered conformational ranges therefore already encompass quite high energies, relative to thermal energies (even at room temperature). The $\pm$ac eclipsed conformation, even at the $\pm 30^\circ$ extremes of its range is considerably higher in energy than the *gauche* minimum, E_g. Substitution of bulky groups in polymethylene chains will tend to make energies of the eclipsed conformations even greater. The sp

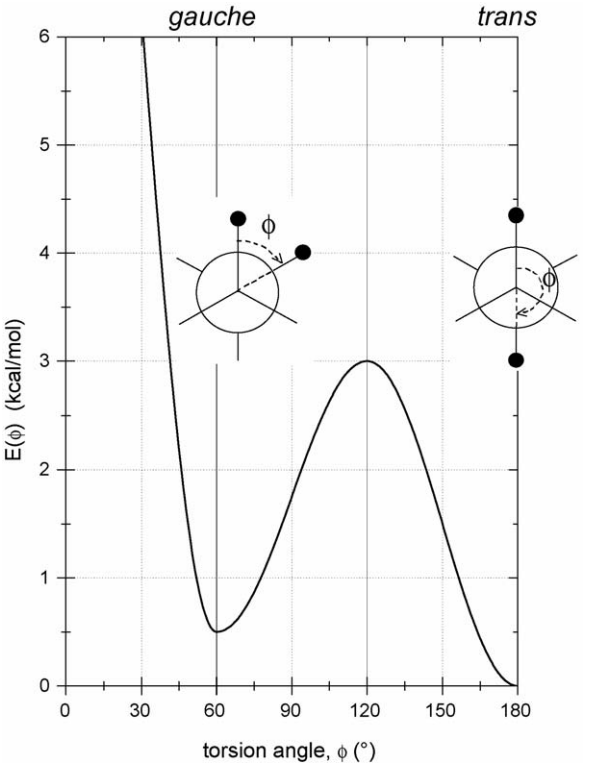

Fig. 2. Schematic dependence of the C–C bond rotational potential, $E(\phi)$, on dihedral torsion angle, ϕ. *Trans* ($\phi = 180°$) and *gauche* ($\phi = 60°$) rotamers are indicated as projections along the C–C bond.

eclipsed conformer is of yet higher energy than the ±ac conformations.

The stable rotamers for a C–C single bond in a lipid chain are, therefore, the three staggered conformations, *trans*, *gauche*$^+$ and *gauche*$^-$ (ap, ±sc). In bilayer crystals of lipids with saturated unbranched fatty acids, the chains are exclusively in the extended, all-*trans* configuration. In the fluid state of lipid membranes, rapid transitions take place between the equilibrium populations of the three staggered rotamers, at a rate of $\geq 10^{10}\,s^{-1}$ (see, e.g., Moser et al., 1989). Eclipsed conformations (±ac) are energetically unfavourable by ca. 3 kcal/mol, and represent the kinetic barriers to rotational isomerism.

The *cis* conformation (sp) is found normally only for C=C double bonds, in unsaturated lipid chains. The C–C single bonds adjacent to a *cis* double bond are conformationally less restricted than those in a saturated chain. Two broad potential minima exist around torsion angles ±110° (extending approximately from ±85° to ±140°) that correspond to the *skew* (ac) conformations. Quasi straight-chain packing can be realised with conformational sequences about the double bond (Δ) of the type $g^+s^+\Delta s^+$ and equivalents (Li et al., 1994). Similar quasi-parallel packing of saturated chains can be achieved if the *gauche* conformations are contained in kink sequences, such as $g^{\pm}tg^{\mp}$ (Träuble, 1971). Adjacent *gauche* conformations of the same sense ($\beta_n/\beta_{n\pm1}$ or $\gamma_n/\gamma_{n\pm1} = g^{\pm}g^{\pm}$) produce a right-angle bend in the all-*trans* chain direction, but are otherwise energetically allowed with $E(g^{\pm}g^{\pm}) \sim 1$ kcal/mol for the pair of bonds (cf. Marsh, 1974). Adjacent *gauche* conformations of opposite sense ($\beta_n/\beta_{n\pm1}$ or $\gamma_n/\gamma_{n\pm1} = g^{\pm}g^{\mp}$) are sterically forbidden for strictly ±60° torsion angles because of the pentane effect. Relatively high local potential minima, however, are found displaced from the $g^{\pm}g^{\mp}$ configuration at torsion angle pairs −65°, 103° and −103°, 65° (Abe et al., 1966). These shallow conformational minima have an energy of $E(g^{\pm}g^{\mp}) \sim 3$ kcal/mol, relative to all-*trans*, E(tt), i.e., approximately half the value per bond of the ±ac eclipsed conformers, E(±ac).

4. Membrane protein crystals

4.1. Lipid backbone and headgroup torsion angles in protein crystals

Table 3 gives the torsion angles determined for a range of phospholipids or glycolipids in crystals of cytochrome *c* oxidase from *P. denitrificans* (Harrenga and Michel, 1999), *Rhodobacter sphaeroides* (Svensson-Ek et al., 2002) and bovine heart (Mizushima et al., 1999); of photosynthetic reaction centres from *Rh. sphaeroides* (McAuley et al., 1999; Fyfe et al., 2000; Camara-Artigas et al., 2002) and *Thermochromatium tepidum* (Nogi et al., 2000); of photosystem I from *Synechococcus elongatus* (Jordan et al., 2001); of light-harvesting complex II from spinach (Liu et al., 2004); of cytochrome *c* reductase from *Saccharomyces cerevisiae* (Lange et al., 2001) and chicken heart (Zhang et al., 1998); of the ADP/ATP exchange carrier from bovine heart mitochondria (Pebay-Peyroula et al., 2003); of the cytochrome b_6f complex from *Mastigocladus laminosus* (Kurisu et al., 2003) and *Chlamydomonas reinhardtii* (Stroebel et al., 2003); of the KcsA K^+-channel from *Streptomyces lividans* (Valiyaveetil et al., 2002); and of formate and succinate dehydrogenases, and nitrate reductase, from *Escherichia coli* (Jormakka et al., 2002; Yankovskaya et al., 2003; Bertero et al., 2003).

In addition to the diacyl lipids phosphatidylcholine (PtdCho), phosphatidylethanolamine (PtdEtn), phosphatidylglycerol (PtdGro), phosphatidylinositol (PtdIns), phosphatidate (Ptd), diglyceride ($acyl_2$Gro), galactosyldiglyceride (Gal(acyl)$_2$Gro), digalactosyl diglyceride (Gal_2(acyl)$_2$Gro), glucosylgalactosyl diglyceride (GlucGal(acyl)$_2$Gro) and sulphoquinovosyl diglyceride (SQ$acyl_2$Gro), data are presented in Table 3

Table 3
Torsion angles (°) of phospholipids/glycolipids in crystals of transmembrane proteins (Marsh and Páli, in press)[a]

Lipid[b]	α_1	α_2	α_3	α_4	α_5	θ_1	θ_2	θ_3	θ_4	β_1	β_2	β_3	β_4	γ_1	γ_2	γ_3	γ_4
Cytochrome *c* oxidase (*P. denitrificans*): PDB:1QLE (Harrenga and Michel, 1999)																	
Ste_2PtdCho	−176	−54	−61	−116	−102	−161	−49	54	−62	−174	−17	132	152	179	−52	142	−122
	179	178	−178	78	155	130	−120	67	−47	131	135	31	−173	178	167	123	179
Cytochrome *c* oxidase (*Rb. sphaeroides*): PDB:1M56 (Svensson-Ek et al., 2002)																	
Ste_2PtdEtn	147	109	176	−173	137	144	−112	−20	−132	−175	153	−128	152	114	92	−167	−179
	−159	32	121	−158	140	−167	−61	155	44	122	−150	−157	158	−166	180	−88	111
	142	−142	−100	151	143	48	162	147	32	122	155	−83	−151	−92	−161	−91	−163
	−156	−75	132	151	174	−54	58	−93	156	80	171	−109	110	−164	153	161	130
	160	−111	−70	−80	151	−115	1	−150	86	99	167	−102	155	−118	−179	160	131
	−164	141	152	−3	−170	133	−107	−129	109	131	100	177	−174	−167	168	175	74
Cytochrome *c* oxidase (bovine): PDB:1V54 (Tsukihara et al., 2003)																	
PalLinPtdCho	−153	−96	98	120	−85	32	162	−127	103	−51	−126	108	−138	−110	120	−80	−84
$Ste\Delta_4$AchPtdEtn	130	−58	108	−145	111	−81	49	47	−85	133	142	118	133	117	−168	172	−100
	−125	−72	−71	−102	165	64	−179	−146	96	133	159	−91	143	−152	151	151	171
	151	−97	−127	177	−69	176	−62	−139	98	127	174	−145	114	−112	−129	166	163
PalVacPtdGro	−140	−69	−59	175	−63	−50	67	−178	63	104	176	167	−178	86	175	42	58
	94	75	85	116	−178	63	−176	−167	75	127	−179	176	84	−107	169	−153	−168
	−91	−92	129	144	−120	−93	34	172	44	106	146	−139	69	165	163	179	150
	52	82	−78	27	−158	89	−125	−64	149	−46	−105	87	−136	−137	−87	−38	98
$(acyl_2Ptd)_2$Gro	150	−74	−31	−135	138	139	−92	−133	99	144	−133	−150	107	−174	107	−72	149
	−96	−119	164	35	118	162	−71	116	−10	122	165	−64	−154	−170	164	−162	−151
	−85	−157	−112	114	−41	114	−124	−144	93	69	120	−92	80	−173	160	99	−177
	153	−76	−7	155	118	134	−105	−118	122	126	142	−97	−176	−116	175	−156	−112
Cytochrome *c* reductase (*S. cerevisiae*): PDB: 1KB9 (Lange et al., 2001)																	
$acyl_2$PtdEtn	163	61	−179	−79	135	−18	104	−180	56	77	180	−92	−80	180	180	29	−136
	142	102	−87	−116	−31	145	−94	179	56	130	170	180	137	179	179	75	−131
$acyl_2$PtdCho	179	−49	−109	139	55	−140	−29	−179	65	136	133	148	129	180	180	73	176
$acyl_2$PtdIns	−151	115	−73	–	–	−65	47	180	61	132	127	167	70	−179	180	−179	109
$(acyl_2Ptd)_2$Gro	180	46	−119	144	51	−116	0	−179	61	110	41	108	167	179	−64	−36	−84
	179	−163	−143	−180	−133	−115	0	180	61	124	118	−141	180	180	161	180	66
Cytochrome *c* reductase (chicken): PDB: 1BCC (Zhang et al., 1998)																	
	122	−61	164	155	−163	−71	108	−113	69	−115	−179	176	180	−134	17	109	123
	−134	−63	−168	−117	−82	−86	93	−51	131	−175	179	176	−179	−113	89	−120	−170
ADP/ATP carrier (bovine): PDB:1OKC (Pebay-Peyroula et al., 2003)																	
$acyl_2$PtdCho	180	−64	−62	−89	−109	117	−128	87	−30	86	147	−1	107	180	−103	−161	160
	−179	−62	−62	−140	−106	−43	72	90	−27	125	150	85	149	180	171	76	−112
	−178	−60	−63	−176	−178	−41	75	171	52	102	180	−107	100	180	110	–	–
	−179	–	–	–	–	−51	63	−143	99	87	149	−112	106	180	156	–	–
$(acyl_2Ptd)_2$Gro	−156	124	−66	−179	−63	123	−123	90	−36	150	155	−74	−169	177	−179	136	94
	118	−65	−158	148	−54	123	−118	180	62	140	133	146	180	167	180	−88	–
	−163	123	−64	−148	−65	15	136	−85	150	132	139	−118	−177	−113	180	–	–
	167	−57	136	−142	−92	−13	108	180	60	137	114	−119	180	106	180	−135	–
	–	–	–	–	–	–	–	50	−81	−59	−116	−146	−83	147	180	168	−162
Photosynthetic reaction centre (*Rb. sphaeroides*): PDB:1M3X, 1QOV, 1E14 (Camara-Artigas et al., 2002; McAuley et al., 1999; Fyfe et al., 2000)																	
$acyl_2$PtdCho	−140	146	−40	−111	167	53	179	179	47	81	103	80	180	180	180	−69	144
(Glc Gal) $acyl_2$Gro	0	–	–	–	–	−62	118	−106	74	0	160	−178	168	180	−162	0	−66
$(acyl_2Ptd)_2$Gro	137	130	−62	−173	−66	97	−142	−151	84	156	142	−152	−156	−147	−177	−145	−156
	−163	−43	−88	173	−59	−58	62	176	58	95	164	−120	180	90	176	84	−144
						−62	59	149	30	97	−174	−120	154	120	163	96	−128
Photosynthetic reaction centre (*Th. tepidum*): PDB:1EYS (Nogi et al., 2000)																	
Pam_2PtdEtn	179	−131	53	−88	99	−98	18	−143	96	62	177	−83	−179	−83	42	180	−64
Photosystem I (*S. elongatus*): PDB:1JB0 (Jordan et al., 2001)																	
Pam_2PtdGro	176	33	179	−141	−156	49	172	74	−50	130	−155	−66	179	153	−146	127	67
	−179	57	−179	157	120	51	169	166	46	102	158	−95	−162	−109	−157	−66	
	179	43	−178	122	−58	−60	60	176	54	120	119	−178	178	122	−109		

Table 3 (*Continued*)

Lipid[b]	α_1	α_2	α_3	α_4	α_5	θ_1	θ_2	θ_3	θ_4	β_1	β_2	β_3	β_4	γ_1	γ_2	γ_3	γ_4
Gal Ste_2Gro	158					67	−176	60	−60	143	−178	−66	−172	179	176	180	−52
Light-harvesting complex II (spinach): PDB:1RWT (Liu et al., 2004)																	
Pam_2PtdGro	−159	−101	−71	−154	−139	91	−151	10	−112	131	−150	−107	−153	123	54	−95	108
	−158	−157	177	−160	−62	135	−107	1	−121	140	−160	−103	−155	120	62	−87	108
	−169	−113	−163	−170	−28	95	−148	0	−123	139	−158	−111	−160	124	63	−94	109
Gal_2Ste_2Gro	−132					161	−79	92	−31	167	170	−156	−136	−120	−107	127	129
Cytochrome b_6f (*M. laminosus*): PDB:1UM3 (Kurisu et al., 2003)																	
Ole_2PtdCho	179	−178	148	178	178	−65	55	−78	165	−176	1	141	180	−140	0	180	−64
	−110	−107	119	178	−176	158	−77	−47	−171	−64	−1	−124	163	−175	−177	−165	−68
	162	85	96	174	174	178	−62	−57	−174	−170	2	144	172	−107	2	−92	−168
	165	−88	103	−168	−176	170	−67	36	−87	−52	0	−148	74	−155	180	38	172
Cytochrome b_6f (*C. reinhardtii*): PDB:1Q90 (Stroebel et al., 2003)																	
Gal Ste_2Gro	142	–	–	–	–	65	−178	152	38	99	−176	57	180	−179	180	180	−170
	−170	–	–	–	–	62	−178	164	41	139	180	−178	180	180	180	180	173
SQ $acyl_2$Gro	144	–	–	–	–	−160	−41	62	−59	108	171	–	–	127	−131	−139	180
Nitrate reductase A (*E. coli*): PDB:1Q16 (Bertero et al., 2003)																	
$acyl_2$PtdGro	−178	59	−147	160	−58	159	−70	180	50	137	169	−170	62	103	146	129	−128
$acyl_2$PtdH	−157	–	–	–	–	−67	112	−76	104	−121	–	–	–	180	170	180	−151
Formate reductase N (*E. coli*): PDB:1KQF (Jormakka et al., 2002)																	
$(acyl_2Ptd)_2$Gro	−138	−136	−178	−73	−31	−12	96	−158	84	101	108	−45	142	105	179	−38	−108
	169	−123	−30	−129	−134	−84	31	−119	121	144	143	−79	−158	−151	144	104	−175
Succinate dehydrogenase (*E. coli*): PDB:1NEK (Yankovskaya et al., 2003)																	
$(acyl_2Ptd)_2$Gro	180	178	180	179	36	177	−65	66	−52	135	−179	−160	−173	152	−133	95	−179
	143	−174	−112	−95	162	−66	53	−112	130	129	−158	−149	180	179	−164	−118	138
$acyl_2$PtdEtn	180	157	−52	131	−168	65	−177	−177	61	93	179	−58	180	−179	180	−76	−172
KcsA channel (*S. lividans*): PDB:1K4C (Valiyaveetil et al., 2002)																	
$acyl_2$Gro	–	–	–	–	–	50	172	164	42	112	75	112	174	−166	163	96	−163

[a] α_i, θ_i, β_i and γ_i are torsion angles of headgroup, glycerol backbone, *sn*-2 chain and *sn*-1/*sn*-3 chain, respectively (see Hauser et al., 1981 and Fig. 1).

[b] Abbreviations: Ptd, phosphatidyl; Cho, choline; Gro, glycerol; Etn, ethanolamine; Ins, inositol; Glc, glucose; Gal, galactose; SQ, sulphoquinovosyl; Ste, stearoyl; Pam, palmitoyl; Phy, phytanyl; Lin, linoleoyl; Vac, vaccenoyl; Δ_4Ach, arachidonoyl.

for the tetraacyl lipid diphosphatidyl glycerol (cardiolipin, $(acyl_2Ptd)_2$Gro). Torsion angles are listed separately for the two phosphatidyl moieties of cardiolipin, i.e., a double entry corresponds to a single cardiolipin molecule. For each phosphatidyl moiety, the torsion angle α_5 corresponds to rotation about the bond adjacent to the central C(OH) in the bridging glycerol of the cardiolipin headgroup (i.e., α_5 for one corresponds to α_6 for the other and vice-versa).

Table 4 gives the torsion angles for the diphytanyl lipids in different crystals of bacteriorhodopsin from the archaeon *Halobacterium salinarum*. The data given for the PDB:1BRR lipids are those from the first X-ray structure in which endogeneous lipids were well resolved (Essen et al., 1998). Two of these are glycolipids. Of the others in Table 4, the data for PDB:1C3W lipids are from one of the highest resolution (1.55 Å) structures reported to date (Luecke et al., 1999). Nonetheless, the headgroup structure was not resolved for these diphytanyl ether-linked lipids. Correspondingly, the diphytanyl glycerol structures with PDB code 1QHJ were modelled into the electron density, but not included in the refinement (Belrhali et al., 1999). The PDB:1QM8 series of lipids is the only one for which phospholipid headgroups are resolved in the lipids associated with bacteriorhodopsin. One is phosphatidylglycerol phosphate, the methylated derivative of which is the major membrane lipid of *H. salinarum*. It is likely that the other phospholipid moieties, phosphatidic acid and phosphatidylglycerol represent fragments of phosphatidylglycerol phosphate methyl ester. Phosphatidylglycerol itself is, however, a minor lipid constitutent of *H. salinarum* (Belrhali et al., 1999; Kates et al., 1993). Diphytanyl glycolipids are also present, as already mentioned, and are designated triglycosyl diphytanylglycerol in Table 4.

4.2. Lipid chain torsion angles in protein crystals

Fig. 3 gives the positional dependence of the hydrocarbon chain torsion angles, γ_n and β_n, for the lipids

Table 4
Torsion angles (°) of diphytanyl phospholipids and glycolipids in crystals of bacteriorhodopsin (Marsh and Páli, in press)[a]

Lipid[b]	PDB	Ref.[c]	α_1	α_2	α_3	α_4	α_5	θ_1	θ_2	θ_3	θ_4	β_1	β_2	β_3	β_4	γ_1	γ_2	γ_3	γ_4
Phy_2Gro	1BRR	1						178	58	170	−71	−112	−157	171	−169	−146	−177	−169	−179
Triglycosyl Phy_2Gro	1BRR	1	38					−128	108	−106	27	−45	89	169	175	−116	−164	−166	175
			110					−162	77	−164	−42	−85	166	145	−168	−166	−172	−175	−176
Phy_2Gro	1C3W	2						63	−179	−10	−128	142	−138	−69	−127	104	132	−124	33
								50	−80	41	171	−115	−25	−138	103	99	−68	155	−118
								−9	−129	83	−158	−115	120	−177	141	108	−30	−100	−166
								49	−70	70	−171	166	117	161	137	86	17	−163	−168
Phy_2Gro	1QHJ	3								153	−63	10	−177	−140	27	−87	−163	−150	−136
										33	179	56	151	−73	−67	74	145	67	−176
										−111	93	104	67	172	168	−136	59	−153	180
										107	−75	−78	−107	107	−151	160	168	−178	162
										133	−74	77	109	69	−141	111	138	167	179
										42	−174	170	79	−161	45	153	147	−163	−166
										51	−150	−103	−71	168	169	77	55	−171	174
										−60	153	59	69	95	−167	−57	−63	170	−167
										−164	51	82	86	170	−55	−177	118	−149	−159
Phy_2Ptd	1QM8	4	98					−160	78	175	−64	−59	−113	−150	175	152	−75	156	−165
Triglycosyl Phy_2Gro	1QM8	4	56					−129	109	−110	10	−46	105	172	179	−105	−158	−167	174
								−86	154	117	−124	154	157	147	100	70	133	−176	−78
$Phy_2PtdGroP$	1QM8	4	164	30	162	166	134	71	−50	165	−74	57	100	−161	173	−172	−172	−165	179
$Phy_2PtdGro$	1QM8	4	−144	−179	50	93	135	−146	91	−170	−51	157	−160	170	−81	178	168	−175	−70

[a] α_i, θ_i, β_i and γ_i are torsion angles of headgroup, glycerol backbone, *sn*-2 chain and *sn*-3 chain, respectively (see Hauser et al., 1981 and Fig. 1).
[b] Abbreviations: Ptd, phosphatidyl; Gro, glycerol; Gro*P*, glycerol phosphate; Phy, phytanyl.
[c] References: 1, Essen et al. (1998); 2, Luecke et al. (1999); 3, Belrhali et al. (1999); 4, Takeda et al. (2000).

in crystals of four different transmembrane proteins. For $n>3$, γ_n and β_n correspond to torsion angles of the purely hydrocarbon section of the chain, undisturbed by the ester or ether linkage. For the two phosphatidylcholine lipids associated with *P. denitrificans* cytochrome *c* oxidase (Harrenga and Michel, 1999), all four chains are 18 C-atoms in length and the torsion angles with $n>3$ correspond to a predominantly *trans* (ap) conformation throughout the chain (Fig. 3A). The latter is especially the case for one of the two molecules, where the mean *trans* torsion angle is $182\pm9^\circ$ (S.D., $N=29$). The only exception to the quasi all-*trans* structure is the single *cis* (sp) conformation $\beta_{13}=0^\circ$, in the *sn*-2 chains of both lipids. This almost certainly corresponds to the presence of a double bond, although all bonds are modelled with bond lengths and bond angles appropriate to C–C single bonds. The bonds adjacent to the C11–C12 *cis* bond are, nevertheless, in the *trans* (ap) conformation, and not in an allowed *skew* conformation.

Fig. 3B gives the chain torsion angles of cardiolipin (diphosphatidyl glycerol, with four chains) in association with a photosynthetic reaction centre mutant from *Rb. sphaeroides*. Not all chains were fully resolved in the electron density, nor could any double bonds be resolved specifically, although expected in the endogenous lipid (McAuley et al., 1999). For the AM260W mutant, the first 14 C-atoms in the *sn*-1 chain and the first 15 C-atoms in the *sn*-2 chain are resolved for one phosphatidyl moiety of diphosphatidyl glycerol. Correspondingly, 15 C-atoms of the *sn*-1 chain and 9 C-atoms of the *sn*-2 chain are resolved for the other phosphatidyl moiety. The cardiolipin chain configuration is predominantly *trans* (ap) in this reaction centre, as for the phosphatidylcholine molecules associated with bacterial cytochrome *c* oxidase. However, the spread in torsion angles is considerably larger (the mean *trans* dihedral is $182\pm16^\circ$ S.D.) for the reaction centre cardiolipin, and a significant proportion of the torsion angles lies in the eclipsed (±ac) range. Only two torsion angles lie within the *gauche* (±sc) range of staggered conformations. None occurs in the *cis* (sp) range, although unsaturated chains are expected in *Rb. sphaeroides* cardiolipins (Russell and Harwood, 1979). Qualitatively similar results (not shown) are found for the cardiolipin molecule associated with the FM197R/GM203D mutant reaction centre (Fyfe et al., 2000). This is of significance because the latter data set was collected at low temperature (100 K), whereas that for the AM260W mutant was obtained at room temperature (298 K).

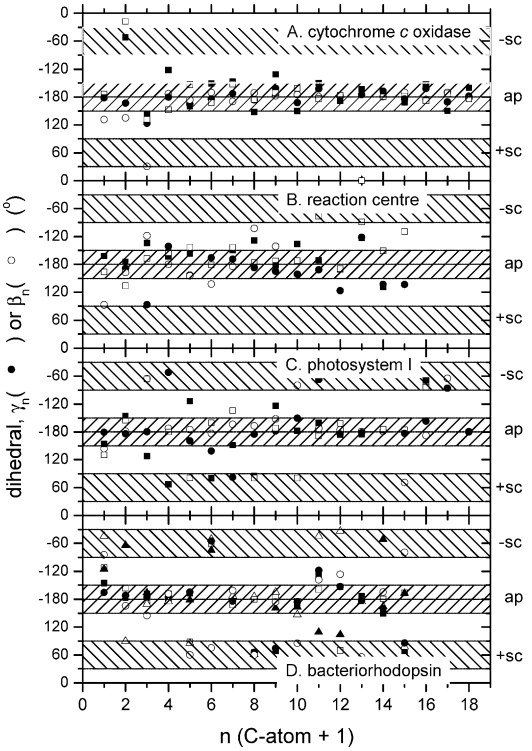

Fig. 3. Positional profiles of the torsion angles, γ_n and β_n, in the *sn*-1/*sn*-3 (solid symbols) and *sn*-2 (open symbols) chains, respectively, of phospho-/glyco-lipids in crystals of integral membrane proteins. (A) Distearoyl phosphatidylcholine in association with *Paracoccus denitrificans* cytochrome *c* oxidase. The two molecules are designated PC2 2 (■, □) and 3 (●, ◯), respectively (Harrenga and Michel, 1999; PDB:1QLE). (B) Cardiolipin in association with *Rhodobacter sphaeroides* photosynthetic reaction centre mutant AM260W (■, □, ●, ◯). The two phosphatidyl moieties are designated CDL A (■, □) and B (●, ◯), respectively (McAuley et al., 1999, PDB:1QOV). (C) Phosphatidylglycerol (LHG) and monogalactosyl diglyceride (LMG) in association with *Synechococcus elongatus* photosystem I (Jordan et al., 2001; PDB:1JB0). The two complete diacyl lipid molecules are LHG 5001 (■, □) and LMG 5002 (●, ◯). (D) Diphytanyl glycerol in association with *Halobacterium salinarum* bacteriorhodopsin. The phytanyl chains of the three molecules are those designated ARC 11 (■), ARC 12 (□), ARC 21 (▲), ARC 22 (△), ARC 31 (●), and ARC 32 (◯) (Essen et al., 1998; PDB:1BRR).

Fig. 3C gives the torsion angles of a phosphatidylglycerol molecule and a monogalactosyl diglyceride molecule in association with the photosystem I complex from *S. elongatus* (Jordan et al., 2001). The phosphatidylglycerol chains are 16 C-atoms in length (i.e., dipalmitoyl) and those of the monogalactosyl diglyceride are 18 C-atoms in length (i.e., distearoyl). The spread in torsion angles for the chains of both lipids is yet greater than that for the cardiolipin acyl chains in contact with the reaction centre. However, the proportion of staggered conformations in Fig. 3C is much higher than in Fig. 3A and B. The greater conformational flexibility arises from an increased population of *gauche* (±sc) rotamers; that of the eclipsed (±ac) rotamers is much lower, particularly for the monogalactosyl diglyceride.

Fig. 3D shows the torsion angles for the chains of three diphytanyl lipid molecules (six chains in total) associated with bacteriorhodopsin (Essen et al., 1998). Each chain is ether-linked to the glycerol backbone, instead of ester-linked as are the chains of the other lipids considered above. The phytanol chain is 16 C-atoms long and fully saturated, but with methyl branches at the 3, 7, 11 and 15 C-atom positions (i.e., a total of 20 C-atoms). Because of the methyl branch at the penultimate carbon of a phytanyl chain, there is ambiguity in defining the final main-chain torsion angle. For this reason, the torsion angles γ_n and β_n in Fig. 3D are defined only up to $n = 15$. The spread in torsion angles of the phytanyl chains interacting with bacteriorhodopsin found in Fig. 3D is qualitatively similar to that found for the diacyl lipids associated with photosystem I. Again, the greater conformational flexibility relative to Fig. 3A and B arises from a greater number of staggered *gauche* (±sc) rotamers, rather than of energetically unfavoured eclipsed (±ac) rotamers. No *cis* (sp) conformers are found, and none are expected for saturated phytanyl chains.

Results from the other three datasets for diphytanyl lipids associated with bacteriorhodopsin are not shown in Fig. 3. These differ considerably from those shown in Fig. 3D in that they contain a considerably higher proportion of eclipsed conformers. For the PDB:1C3W series, the population of eclipsed (±ac) conformers equals that of the *trans* (ap) conformers, and the proportion of *gauche* (±sc) conformers is rather low. The PDB:1QHJ and PDB:1QM8 series are both characterised by an appreciable population of eclipsed (±ac) conformers, and also of *gauche* (±sc) conformers. Again, *cis* (sp) conformers are almost absent.

5. Comparison of lipid conformations in membranes and protein crystals

Many of the lipid chain configurations in protein crystals are characterised by a relatively high proportion of energetically unfavourable eclipsed conformations (Marsh and Páli, in press). In principle, rather high rotational conformational energies, can be sustained in the lipid molecules if there is a compensating energetically favourable stabilisation by the lipid–protein interaction. In this scenario, the surface contour of the hydrophobic protein side chains would force the lipid into eclipsed conformations in order to optimise their mutual interactions. Measurements on the selectivity of lipid–protein

interactions with rhodopsin and other membrane proteins reveal only a weak dependence on lipid chain length (Ryba and Marsh, 1992; Marsh, 1995). This implies that the interaction of lipid chains with the hydrophobic surface of transmembrane proteins is only marginally more favourable than the interaction of lipid chains with themselves. In further support of this, little selectivity is found between spin-labelled lipids of the same headgroup but different numbers of chains in the interaction with cytochrome *c* oxidase and with the Na, K-ATPase (Powell et al., 1987; Esmann et al., 1988). Finally, the off-rates for exchange of non-selective lipids at the intramembranous surface of integral proteins, although significantly slower, are nevertheless comparable to diffusive lipid–lipid exchange rates in fluid lipid bilayers (Marsh and Horváth, 1998). This again implies no strong preferential interaction of the lipid chains with the protein rather than with themselves.

The results of spectroscopic thermodynamic studies therefore suggest that lipid chains have affinities among themselves that are energetically similar to those for the lipid–protein interface. Typically chain cohesions in fluid lipid bilayers correspond to interaction free energies of $\Delta G_n \sim -0.6$ kcal/mol/CH_2 (Cevc and Marsh, 1987; King and Marsh, 1987). The preferential selectivities for the lipid–protein interface, determined as mentioned above, are approximately one-tenth of this (Marsh and Horváth, 1998). A possible exception is cardiolipin interacting with the ADP–ATP carrier, for which the off-rate of lipid exchange is considerably lower than would be predicted from the average relative association constant (Horváth et al., 1990). On balance, these measurements therefore suggest that lipid chain interactions with integral proteins in membranes are unlikely to produce sufficient stabilisation energy to compensate the formation of energetically unfavourable eclipsed conformations.

It is possible that the energetic considerations above regarding generalised lipid–protein interactions in membranes may not apply to the lipids that are resolved specifically in the X-ray structures of membrane protein crystals. Much stronger stabilisation of the lipid–protein interaction may be required or indicated in the latter case. This cannot, however, apply universally to cases in which all lipids at the protein interface are resolved (e.g., Belrhali et al., 1999). Further, very few eclipsed conformations are present in structures for which the mean temperature factors (B-values) of the lipids are comparable to those of the protein. This is also true for the protein side chains in high-resolution crystal structures (Ponder and Richards, 1987). Both these facts suggest rather strongly that the conformational violations in the lipids may well be the result of configurational disorder rather than representing true molecular structures (see also DePristo et al., 2004).

Table 5
Classification of glycerolipid structures in membrane protein crystals according to backbone configuration (Marsh and Páli, in press)[a]

θ_4/θ_2	(θ_3/θ_1)	N^b	Rel. population (%)
Staggered, parallel-chain			
sc/sc	(tg^-)	10	9
−sc/−sc	(g^+t)	9	9
	(tg^+)	1	
sc/ap	(tg^+)	11	10
−sc/ap	(g^+g^+)	2	2
sc/−sc	(tt)	5	4
−sc/sc	(g^+g^-)	2	5
	(tt)	4	
Staggered, nonparallel-chain			
ap/−sc	(g^-t)	2	4
	(g^+g^+)	2	
ap/sc	(g^-g^-)	3	2
Eclipsed		62	55

[a] For definition of torsion angles see Fig. 1.
[b] Number of structures.

5.1. Glycerol backbone configuration

Table 5 groups the various lipid structures in membrane protein crystals according to their θ_4/θ_2 and θ_3/θ_1 torsion angle configurations. Combinations of these complementary torsion angle pairs are given appropriate to the expected optical enantiomer for non-archaea and archaea. Because the interaction of the lipid chains with the hydrophobic protein side chains removes the necessity for the strictly parallel chain stacking that is found in lipid crystals, a leading chain cannot always be identified unambiguously. Therefore, this classification is not attempted. Thirty-five percent of the structures have staggered configurations that are found with parallel chain stacking in the crystals of phospholipids (cf. Table 2). A further five structures of archaeal lipids have corresponding configurations but of the opposite optical enantiomer. Seven of the structures have staggered configurations that would not give rise to parallel chain stacking in bilayers and therefore are not represented in the phospholipid crystals. All of the remaining structures have at least one eclipsed conformation and 42% of these have both torsion angles in the eclipsed range.

The staggered, parallel-chain structures for non-archaeal lipids in the protein crystals comprise 26% sc/sc, 23% −sc/−sc, 28% sc/ap, 5% −sc/ap and 13% sc/−sc configurations, together with 5% of the −sc/sc

enantiomer. In the lipid crystals, the relative occurrences are, for comparison: 36% sc/sc, 18% −sc/−sc, 6% sc/ap, 9% −sc/ap and 30% sc/−sc (Table 2). Thus, the protein-interacting lipids are relatively enriched in conformations with θ_2 = ap, at the expense of the sc/−sc conformer. Presumably, protein–lipid interactions outweigh the intramolecular "gauche effect" in the more abundant sc/ap structures. Indeed, both secretory and pancreatic phospholipases A_2 bind inhibitory substrate analogues in the sc/γ/ap configuration (Scott and Sigler, 1994; Thunnissen et al., 1990).

As already mentioned, lipids at the protein interface must not necessarily display the parallel chain packing that is essential in bilayer crystals. Therefore, the ap/−sc configurations in Table 5 are not automatically disfavoured sterically. In fact, departures from parallel chain packing may be required in some instances if both chains are to be accommodated in grooves in the protein surface. There are examples of nonparallel-chain structures also for phospholipids in the binding sites of soluble proteins (Pascher, 1996; Marsh, 2003). Phosphatidylcholine bound as an inhibitor of the pancreatic lipase–colipase complex adopts the ap/sc configuration (van Tilbeurgh et al., 1993). On the other hand, a phosphocholine analogue takes up the ap/ap glycerol configuration as inhibitor complex with cobra venom phospholipase A_2 (Plesniak et al., 1995).

It has been suggested, on the basis of evidence summarised earlier above, that the sc/γ conformer predominates in the dynamic configuration of glycerolipids in hydrated bilayer membranes (Pascher, 1996). This permits all three θ_2 rotamers of the headgroup. The lipids associated with membrane proteins in their crystals apparently sample a wider conformational space. Of the conformations found in lipid bilayer crystals, all are fully represented by lipids in the crystals of membrane proteins.

5.2. Lipid chain configuration

The eucaryotic and bacterial lipids contain a rather large proportion of eclipsed *skew* conformers, at the expense of *gauche* conformers (see, e.g., Fig. 3A–C). For those chains with appreciable *gauche* populations, only six classical g^+tg^- kink sequences are found (Fig. 3C); 19 $g^{\pm}g^{\pm}$ sequences appear in the complete range of lipids surveyed in Tables 3 and 4, and five g^-g^+ sequences occur at the chain ends (where they are sterically allowed). Interestingly, several of these coupled sequences (6 out of 30) appear in just two lipids: both are dioleoyl phosphatidylcholines associated with *M. laminosus* cyt b_6f (Kurisu et al., 2003).

The single *cis* conformation of phosphatidylcholines associated with *P. denitrificans* cytochrome *c* oxidase (Harrenga and Michel, 1999) (see Fig. 3A) is in the *sn*-2 chain, as expected for a *cis* double bond. The location of the putative unsaturated cΔ-bond is at the C11–C12 position, rather than at the C9–C10 position as in oleic acid, the common monounsaturated fatty acid. Flanking *skew* conformations such as might facilitate straight-chain packing are also absent. Otherwise, the phosphatidylcholine chains associated with *P. denitrificans* cytochrome oxidase are predominantly in the *trans* configuration, corresponding to a rather pronounced ordering at the lipid–protein interface. *Gauche* conformations apparently are absent and the proportion of energetically unfavourable eclipsed conformations (which might indicate the presence of non-identified *gauche* conformations) is rather low, especially for one of the two molecules. For phosphatidylcholine associated with *Rb. sphaeroides* reaction centre (Camara-Artigas et al., 2002), the *sn*-2 *cis* bond is in the position expected for oleic acid; but for glucosyl galactosyl diglyceride also associated with the reaction centre, the *cis* bond is at position C8–C9 of the lipid chain and is flanked by *trans* rather than by *skew* conformers. The chains of these two lipids are also almost devoid of *gauche* rotamers, but disorder is introduced by a limited number of *skew* conformations. This is also the case for the resolved chain segments of phosphatidylcholine associated with *S. cerevisiae* cytochrome *c* reductase (Lange et al., 2001).

The chains of cardiolipin, phosphatidylethanolamine, phosphatidylcholine and phosphatidylglycerol associated with bovine cytochrome *c* oxidase (Tsukihara et al., 2003) contain *cis* (sp) conformers, presumably associated with double bonds. All four chains of each cardiolipin have C9–C10 and C12–C13 *cis* rotamers corresponding to the C18:2c$\Delta^{9,12}$ configuration of linoleic acid which constitutes nearly all chains of cardiolipin associated with bovine cytochrome *c* oxidase (Powell et al., 1985). The *sn*-2 chains of phosphatidylethanolamine have *cis* torsion angles, β_7, β_{10}, β_{13} and β_{16}, about the C5–C6, C8–C9, C11–C12 and C14–C15 bonds which correspond to the C20:4c$\Delta^{5,8,11,14}$ configuration of arachidonic acid. The *sn*-2 chains of phosphatidylglycerol have a *cis* configuration about the C11–C12 bond, which corresponds to C18:1cΔ^{11}, i.e., the *cis* rather than the usual *trans* double bond of vaccenic acid. The *sn*-2 chains of phosphatidylcholine have *cis* β_{11} and β_{16} torsion angles that would correspond to a C18:2c$\Delta^{9,14}$ configuration, although the PDB:1V54 file describes this as a linoleoyl chain. Of the 34 double bonds in the phospholipids associated with bovine cytochrome

c oxidase, 65% have at least one adjacent *skew* (ac) conformation, and 35% have two adjacent *skew* conformers. These, however, account for only 24% of the total *skew* conformations in the chains of these lipids.

The chains of one phosphatidylglycerol, and of galactosyl diglyceride, associated with *S. elongatus* PS I (Jordan et al., 2001) contain no *cis* bonds (see Fig. 3C). Conformational disorder is restricted mostly to *gauche* rotamers, with the population of eclipsed conformers being very low. The chains of phosphatidylglycerol and of digalactosyl diglyceride associated with spinach LHC II (Liu et al., 2004) also contain no *cis* bonds. However, the population of *skew* conformers in these chains is very high.

The *cis* (sp) conformers that appear in phosphatidylethanolamines associated with *Rb. sphaeroides* cytochrome *c* oxidase (Svensson-Ek et al., 2002) are confined to the *sn*-1 chain and largely appear in unconventional positions. They therefore likely correspond to energetically forbidden eclipsed conformers. Both *sn*-1 and *sn*-2 chains contain a high proportion of the energetically disallowed *skew* (ac) conformers that are not associated with double bonds. Similar considerations apply to phosphatidylethanolamine associated with the *Th. tepidum* reaction centre (Nogi et al., 2000), although here the $\gamma_6 = \mathrm{sp}$ *cis* conformer is flanked by *skew* (−ac) conformers. The only *cis* conformer in the phosphatidylethanolamines associated with *S. cerevisiae* cytochrome *c* reductase (Lange et al., 2001) is $\gamma_{10} = \mathrm{sp}$ in a single *sn*-1 chain. The population of eclipsed *skew* conformers is rather high, however, 44% ±ac for both phosphatidylethanolamines. That for phosphatidylinositol, which contains no *cis* conformers is less: 30% ±ac, although still considerable. Phosphatidylethanolamine associated with *E. coli* succinate dehydrogenase (Yankovskaya et al., 2003) also conforms to this general pattern: 36% ±ac and no sp.

Although the four lipids associated with the *M. laminosus* dimer cytochrome b_6f complex are designated as dioleoyl phosphatidylcholine (used in the crystallisation; Kurisu et al., 2003), only two of the eight chains contain a *cis* rotamer. Further, these two *cis* conformers are at the C8–C9 position of the chain, rather than at the C9–C10 position of the *cis* double bond in oleic acid. The chain disorder of these phosphatidylcholines is characterised by a rather large population of *gauche* conformers (21%), relative to the energetically disallowed *skew* conformers (7%). All four lipids, however, contain an unconventional methyl substitution at the C2 position of the glycerol backbone. This additional methyl group is not present in dioleoyl phosphatidylcholine, nor in any known naturally occurring glycerolipid.

The cardiolipins associated with *Rb. sphaeroides* reaction centre (McAuley et al., 1999; Fyfe et al., 2000; Camara-Artigas et al., 2002), *E. coli* formate reductase (Jormakka et al., 2002), and *E. coli* succinate dehydrogenase (Yankovskaya et al., 2003), contain no *cis* conformers in their chains and also very few, or no, *gauche* rotamers. Cardiolipin associated with the reaction centre contains a large proportion (ca. 40%) of eclipsed ±ac conformers, as to a lesser extent does that associated with formate reductase (30% ±ac), whereas that associated with succinate dehydrogenase is characterised by a high *trans* population (76%) and 19% ±ac. On the other hand, cardiolipin associated with *S. cerevisiae* cytochrome *c* reductase (Lange et al., 2001) has two *cis* conformers, at C5–C6 in one phosphatidyl moiety and at C9–C10 in the other, but both in the *sn*-1 chain. This cardiolipin is also characterised by a relatively high *gauche* rotamer population (22% ±sc) and a similar proportion of eclipsed conformers (22% ±ac).

5.3. Phytanyl chain configurations

The branched methyl groups in the phytanyl chains of the archaebacteria have several effects on the stability of the C–C rotamers (see e.g., Flory, 1969). The barrier height associated with the eclipsed conformers is increased. The *trans* configuration of an adjacent bond is increased in energy to be comparable to that of a *gauche* conformer in an unsubstituted chain. The energy of one of the two *gauche* rotamers is increased, relative to that in the unsubstituted chain, by a factor of two or more. For the *R*-configuration of the methyl branches, the most stable configuration for the bonds flanking the substituted C-atom is: g^+t or tg^-, as evidenced by the helical configuration of crystalline polypropylene. The presence of the methyl branches is therefore expected to increase the *gauche* population.

The chains of the lipids associated with bacteriohodopsin in PDB file 1BRR (Essen et al., 1998) have a high proportion of *gauche* rotamers (35% ±sc), consistent with the expectation for phytanyl chains (see Fig. 3D). The population of *skew* (±ac) conformers is also relatively low. Not all *gauche* rotamers are associated with the methyl-substituted C-atoms (i.e., β_4, β_5; β_8, β_9; β_{12}, β_{13}; β_{16}; and similarly for γ), however, and the sense of the *gauche* rotation is not always consistent with the enantiomeric configuration. (Note that all of the PDB:1BRR lipids have the incorrect *S*-configuration.) It is probable that steric interactions of the branched methyl groups with the protein may also tend to increase the population of *gauche* rotamers. The other phytanyl-chain lipids associated with bacte-

riorhodopsin (PDB:1C3W, 1QHJ and 1QM8; Luecke et al., 1999; Belrhali et al., 1999; Takeda et al., 2000) have a considerably higher population of the disallowed, *skew* eclipsed conformations than do the PDB:1BRR lipids. With the exception of the PDB:1C3W lipids, however, they do also have a relatively high *gauche* population, in line with expectation for methyl-branched chains. The PDB:1QM8 series of lipids have the correct *R*-configuration for the branched methyl group. However, only one out of six flanking gt/tg combinations (from a total of 23) has the correct sense, viz., $\gamma_8/\gamma_9 = g^+t$. For the PDB:1BRR lipid chains, the high *gauche* population has associated with it neighbouring *gauche* pairs: four $g^{\pm}g^{\pm}$, but also two sterically forbidden g^+g^- combinations (see Fig. 3D). The latter is not the case for the other lipid series associated with bacteriorhodopsin, although $g^{\pm}g^{\pm}$ pairs are relatively abundant in the PDB:1QHJ lipids.

5.4. Headgroup configuration

Of the various headgroup conformers in Tables 3 and 4, only that for the B moiety of cardiolipin associated with the *Rb. sphaeroides* photosynthetic reaction centre (PDB:1QOV, 1M3X; McAuley et al., 1999; Camara-Artigas et al., 2002) conforms completely to the configuration found in single crystals of phospholipids. At the protein interface, the range of polar group orientations and conformations is much wider than in lamellar crystals of diacyl phospholipids or in fluid phospholipid bilayer membranes (compare Tables 3 and 4 with Table 2). In nearly all cases, the lipid phosphate is anchored by hydrogen bonding to protein residues. For all protein-associated phospholipids, with the exception of one cardiolipin and one phosphatidylglycerol associated with bovine cytochrome *c* oxidase (PDB:1V54, Tsukihara et al., 2003), the α_1-torsion angle is either ap or $\mp$ac, as found in phospholipid crystals. Only eight headgroup structures have the energetically most favourable $\alpha_2/\alpha_3 = \pm$sc/$\pm$sc configuration for the phosphate diester, and a further 10 have the next most favourable $\alpha_2/\alpha_3 = \pm$sc/ap configuration. Several of the lipids have an energetically disfavoured eclipsed conformation for the α_5-torsion angle (Tables 3 and 4).

One of the two distearoyl phosphatidylcholine molecules associated with *P. denitrificans* cytochrome *c* oxidase has the headgroup configuration found in bilayer crystals, except that the C–C torsion angle α_5 is in the energetically unfavourable $-$ac eclipsed conformation (see Table 3), because of interaction with Asp 124(C). The headgroup configuration of the other phosphatidylcholine molecule, by contrast, is very different. It extends away from the acyl chains, with all torsion angles except α_4 in the ap conformation, presumably because of steric and hydrophobic interactions with the protein side chains. Thus, the phosphate diester (α_2/α_3 = ap/ap) does not have the energetically preferred $\pm$sc/$\pm$sc configuration, but α_5 is staggered rather than eclipsed in this molecule. The headgroups of the phosphatidylcholine molecules associated with bovine cytochrome *c* oxidase are also extended away from the chains, although the conformers are largely anticlinal rather than ap. Phosphatidylcholine associated with the *Rb. sphaeroides* reaction centre, and also with *S. cerevisiae* cytochrome *c* reductase, has one phosphate diester torsion angle in the energetically unfavourable ac conformation. Otherwise, the torsion angles conform to those found in phospholipid crystals, but the headgroup deviates somewhat from the fully bent-down orientation. None of the four phosphatidylcholines associated with the cytochrome b_6f complex have the preferred $\pm$sc/$\pm$sc configuration of the phosphate diester. The headgroups of these lipids are extended away from the chains in two cases, or are extended in a direction perpendicular to the chains in the other two cases. All four lipids are located in cavities at the dimer interface.

Phosphatidylethanolamine associated with the *Th. tepidum* photosynthetic reaction centre has a headgroup configuration that departs from the energetically preferred conformations. The torsion angle α_2 of the phosphate diester is $-$ac rather than +sc, and the α_5 = +ac C–C torsion angle is eclipsed. The headgroup is bent down towards the chains with the N-atom hydrogen-bonded to the backbone of Gly 256(M).

One of the two phosphatidylethanolamines associated with *S. cerevisiae* cytochrome *c* reductase has the second most favourable (sc/ap) configuration for the phosphate diester. The torsion angle $\alpha_4 = -$sc is *gauche* and that of α_5 = ac is eclipsed. This brings the headgroup N-atom within hydrogen bonding distance of Glu 24(G). The other resolved phosphatidylethanolamine, has an α_2 = ac configuration, instead of $-$sc. Otherwise, torsion angles are in the ranges found in phospholipid crystals. For both phosphatidylethanolamine molecules, the headgroup is directed away from the chains. Phosphatidylethanolamine associated with *E. coli* succinate dehydrogenase has an ap/$-$sc configuration of the phosphate diester and torsion angles, otherwise, are those found in phospholipid crystals. The headgroup is bent down over the chains in a lipid-bilayer compatible configuration.

The six phosphatidylethanolamines associated with *Rb. sphaeroides* cytochrome *c* oxidase display a variety of different headgroup configurations that are directed

away from the chains, to a greater or lesser extent, in different orientations. The torsion angles differ considerably between the different molecules, and from those in phospholipid crystals, although the α_1 torsion angle is ap (with one exception), and predominantly the α_4 torsion angle is also ap. None of the phosphate diester torsion angles correspond to the energetically favourable configurations. The phosphatidylethanolamines associated with bovine cytochrome *c* oxidase also display a variety of headgroup conformations. Two equivalent headgroups are extended away from the chains and are involved in H-bonding to the protein, whereas those of the other two pairs are bent down, and one of these is also involved in H-bond formation.

The three dipalmitoyl phosphatidylglycerol molecules associated with photosystem I have an α_1 = ap torsion angle as for phosphatidylcholine/ethanolamine in bilayer crystals, rather than the ±ac conformation found in crystals of dimyristoyl phosphatidylglycerol. Also, the second torsion angle of the phosphate diester is in the α_3 = ap conformation, rather than the expected +sc conformation (compare Tables 2 and 3). The α_4 torsion angles of two of the phosphatidylglycerol molecules are ±ac, as in the lipid crystals, whereas that of the third is the allowed ap conformation. The α_5 C–C torsion angle of one phosphatidylglycerol has the ap conformation as in the lipid crystal, that of another is the staggered −sc conformer, whereas the remaining one has an eclipsed conformer. The oxygen $\alpha_{5O/O}/\alpha_{6O/O}$ torsion angles are +sc/+sc, −ac/−sc and ap/−ac for the three molecules, respectively. Thus, two headgroups have the natural 1-*sn* configuration, but the third has the incorrect 3-*sn*-glycerol headgroup enantiomer. All other non-archeal phosphatidylglycerol headgroups are the correct 1-*sn* enantiomer with mean values of α_5–$\alpha_{5O/O} = +122 \pm 2^\circ$ and α_6–$\alpha_{6O/O} = -122 \pm 2^\circ$ ($N = 21$).

Seven out of the 10 phosphatidylglycerol molecules associated with spinach LHC II have a more extended headgroup conformation than in bilayer crystals. The concensus structure is: α_1 = ap, α_2 = ap, α_3 = ap, α_4 = ap, α_5 = −sc and α_6 = +ac. The remaining three phosphatidylglycerol molecules have a different concensus structure: α_1 = ap, α_2 = −ac, α_3 = −sc, α_4 = ap, α_5 = −ac and α_6 = +ac, that approximates somewhat more to the bilayer configuration. The phosphatidylglycerols associated with bovine cytochrome *c* oxidase display a variety of headgroup conformations. With the exception of one equivalent pair, the headgroups are directed away from the hydrocarbon chains, to a greater or lesser extent. Those of two pairs of equivalent molecules are involved in hydrogen bonding to the protein.

The single diphytanyl phosphatidylglycerol and diphytanyl phosphatidylglycerol phosphate molecules associated with bacteriorhodopsin in the PDB:1QM8 structure (Takeda et al., 2000) have headgroup configurations that bear no similarity to those in dimyristoyl phosphatidylglycerol crystals (compare Tables 2 and 4). In both molecules, the α_5 C–C torsion angle is in the energetically unfavourable +ac eclipsed conformation, and neither have the energetically favourable +sc/+sc combination for the α_2/α_3 torsion angles. The oxygen torsion angles are $\alpha_{5O/O}/\alpha_{6O/O}$ = −ac/−ac for both, corresponding to the 3-*sn*-glycerol enantiomer, as expected for phosphatidylglycerol and phosphatidylglycerol phosphate from archaea (Joo and Kates, 1969).

In the diphosphatidylglycerol molecule associated with the *Rb. sphaeroides* reaction centre, the torsion angle $\alpha_{5O/O}$ is ap for the A phosphatidyl moiety and +sc for the B phosphatidyl moiety. Thus, the headgroup glycerol is the *sn*-1 enantiomer with respect to the A moiety and *sn*-3 enantiomer with respect to the B moiety of the cardiolipin molecule. Otherwise, the headgroup configuration of the B-phosphatidyl moiety more closely resembles that of DMPG A in lipid crystals (see Tables 2 and 4). The α_2/α_3 = −sc/−sc combination for the B-phosphodiester is energetically more favourable than the +ac/−sc combination for the A phosphodiester. For both A and B sections of the glycerol moiety: α_4 = ap and α_5 = −sc. Of the other diphosphatidylglycerol molecules, only the A moiety of one pair associated with bovine cytochrome *c* oxidase has the energetically favourable ±sc/±sc configuration for the phosphate diester, and none have the next most favourable α_2/α_3 = ±sc/ap configuration. Otherwise, the cardiolipin headgroup torsion angles conform mostly with those found in phospholipid crystals, but with certain exceptions, which have an $\alpha_5 = \mp$ac eclipsed conformation. The headgroup conformation of all cardiolipins in membrane protein crystals is such that the chains of the two diacyl moieties are roughly parallel, as required in a bilayer membrane.

6. Conclusion

The lipids associated with integral proteins in crystals have survived both the solubilisation and purification processes, as well as crystallisation procedures. Routinely, integral proteins solubilised in non-ionic detergents retain part of the endogeneous lipid in the protein-containing mixed micelles. Only after exhaustive exchange against a large excess of exogeneous lipid in a mild detergent such as cholate can all endogeneous lipids be replaced (Warren et al., 1974; Hesketh

et al., 1976). In this way, for instance, it was possible to replace the endogeneous cardiolipin that co-purifies with cytochrome *c* oxidase (Powell et al., 1985; Watts et al., 1978), even though this mitochondria-specific lipid is found in crystals of the purified bovine protein (see Table 3) and is able to enhance the activity of the lipid-substituted enzyme (Abramovitch et al., 1990). By contrast, NMR experiments with deuterated lipids reveal that the major lipid population contacting the protein exchanges rapidly with the fluid bilayer pool (Oldfield, 1982; Bienvenue et al., 1982; Meier et al., 1987; Seelig et al., 1982). Electron spin resonance experiments with spin-labelled lipids put the off-rates for exchange in the region of ca. 1–10 MHz, depending on the affinity of the protein for a particular lipid (Marsh and Horváth, 1998). There are, therefore, grounds to expect that the lipids that are resolved in protein crystals might correspond to special structures that are not necessarily representative of the overall population of first-shell lipids at the protein interface. This interpretation is supported by the occurrence of headgroup configurations that differ widely from those in bilayer membranes.

Examination of the locations of the lipids at the protein interface reveals certainly that some, but not all, of the lipids in protein crystals are found in specialised sites. For example, the six unique lipids resolved in crystals of *Rb. sphaeroides* cytochrome *c* oxidase are located at well-defined positions, in a cleft formed by the two-helix bundles of subunit III, or at the interface between subunit IV and subunits I/III (Svensson-Ek et al., 2002). One pair of cardiolipins associated with the bovine cytochrome *c* oxidase dimer is trapped within the contact sites between the two monomers. In yeast cytochrome *c* reductase, one of the phosphatidylethanolamines is located at the dimer interface, and the phosphatidylinositol occupies a unique interhelical position (Lange et al., 2001). On the other hand, the several lipids resolved in crystals of bacteriorhodopsin are not trapped between helices or within the protein, rather they are positioned around the protein perimeter (Belrhali et al., 1999). Also, the cardiolipin molecules that are resolved in the crystals of bacterial reaction centres are located at the surface of the protein (Fyfe et al., 2001), as are the cardiolipin and one phosphatidylethanolamine associated with yeast cytochrome *c* reductase (Lange et al., 2001).

Stereochemical violations and the occurrence of energetically disallowed rotamers for many lipid structures in the PDB remain causes for concern. Whereas the latter could be indicative of conformational heterogeneity (see also DePristo et al., 2004), incorrect enantiomeric configurations point to deficiencies in the refinement procedure that most probably result from the use of inadequate restraint libraries (Kleywegt et al., 2003).

References

Abe, A., Jernigan, R.L., Flory, P.J., 1966. Conformational energies of *n*-alkanes and the random configuration of higher homologs including polymethylene. J. Am. Chem. Soc. 88, 631–650.

Abe, A., Mark, J.E., 1976. Conformational energies and the random-coil dimensions and dipole-moments of the polyoxides $CH_3\ O[(CH_2)_yO]_xCH_3$. J. Am. Chem. Soc. 98, 6468–6476.

Abramovitch, D.A., Marsh, D., Powell, G.L., 1990. Activation of beef heart cytochrome oxidase by cardiolipin and analogues of cardiolipin. Biochim. Biophys. Acta 1020, 34–42.

Belrhali, H., Nollert, P., Royant, A., Menzel, C., Rosenbusch, J.P., Landau, E.M., Pebay-Peyroula, E., 1999. Protein, lipid and water organization in bacteriorhodopsin crystals: a molecular view of the purple membrane at 1.9 Å resolution. Structure 7, 909–917.

Bertero, M.G., Rothery, R.A., Palak, M., Hou, C., Lim, D., Blasco, F., Weiner, J.H., Strynadka, N.C.J., 2003. Insights into the respiratory electron transfer pathway from the structure of nitrate reductase. Nat. Struct. Biol. 10, 681–687.

Bienvenue, A., Bloom, M., Davis, J.H., Devaux, P.F., 1982. Evidence for protein-associated lipids from deuterium nuclear magnetic resonance studies of rhodopsin–dimyristoylphosphatidylcholine recombinants. J. Biol. Chem. 257, 3032–3038.

Borisova, N.P., Vol'kenshtein, M.V., 1961. Internal rotation in propane and *n*-butane. Zh. Strukt. Khim. 2, 437–442.

Camara-Artigas, A., Brune, D., Allen, J.P., 2002. Interactions between lipids and bacterial reaction centers determined by protein crystallography. Proc. Natl. Acad. Sci. U.S.A. 99, 11055–11060.

Cevc, G., Marsh, D., 1987. Phospholipid bilayers. Physical Principles and Models, Wiley/Interscience, New York.

Chandrasekhar, I., Kastenholz, M., Lins, R.D., Oostenbrink, C., Schuler, L.D., Tieleman, D.P., van Gunsteren, W.F., 2003. A consistent potential energy parameter set for lipids: dipalmitoylphosphatidylcholine as a benchmark of the GROMOS96 45A3 force field. Eur. Biophys. J. 32, 67–77.

DePristo, M.A., de Bakker, P.I.W., Blundell, T.L., 2004. Heterogeneity and inaccuracy in protein structures solved by X-ray crystallography. Structure 12, 831–838.

Elder, M.P., Hitchcock, P., Mason, R., Shipley, G.G., 1977. A refinement analysis of the crystallography of the phospholipid, 1,2-dilauroyl-DL-phosphatidylethanolamine, and some remarks on lipid–lipid and lipid–protein interactions. Proc. R. Soc. Lond. A 354, 157–170.

Esmann, M., Powell, G.L., Marsh, D., 1988. Spin label studies on the selectivity of lipid–protein interaction of cardiolipin analogues with the Na^+/K^+-ATPase. Biochim. Biophys. Acta 941, 287–292.

Essen, L.-O., Siegert, R., Lehmann, W.D., Oesterhelt, D., 1998. Lipid patches in membrane protein oligomers: crystal structure of the bacteriorhodopsin–lipid complex. Proc. Natl. Acad. Sci. U.S.A. 95, 11673–11678.

Ferguson, A.D., Welte, W., Hofmann, E., Lindner, B., Holst, O., Coulton, J.W., Diederichs, K., 2000. A conserved structural motif for lipopolysaccharide recognition by procaryotic and eucaryotic proteins. Struct. Fold. Des. 8, 585–592.

Flory, P.J., 1969. Statistical Mechanics of Chain Molecules. Wiley, London/New York.

Fyfe, P.K., McAuley, K.E., Rothmann, M., Isaacs, N.W., Cogdell, R.J., Jones, M.R., 2001. Probing the interface between membrane

proteins and membrane lipids by X-ray crystallography. Trends Biochem. Sci. 26, 106–112.

Fyfe, P.K., Ridge, J.P., McAuley, K.E., Cogdell, R.J., Isaacs, N.W., Jones, M.R., 2000. Structural consequences of the replacement of glycine M203 with aspartic acid in the reaction center from *Rhodobacter sphaeroides*. Biochemistry 39, 5953–5960.

Gorenstein, D.G., Kar, D., 1977. Effect of bond angle distortion on torsional potentials. Ab initio and CNDO/2 calculations on dimethoxymethane and dimethyl phosphate. J. Am. Chem. Soc. 99, 672–677.

Harlos, K., Eibl, H., Pascher, I., Sundell, S., 1984. Conformation and packing properties of phosphatidic acid—the crystal structure of monosodium dimyristoylphosphatidate. Chem. Phys. Lipids 34, 115–126.

Harrenga, A., Michel, H., 1999. The cytochrome *c* oxidase from *Paracoccus denitrificans* does not change the metal center ligation upon reduction. J. Biol. Chem. 274, 33296–33299.

Hauser, H., Pascher, I., Pearson, R.H., Sundell, S., 1981. Preferred conformation and molecular packing of phosphatidylethanolamine and phosphatidylcholine. Biochim. Biophys. Acta 650, 21–51.

Hauser, H., Pascher, I., Sundell, S., 1988. Preferred conformation and dynamics of the glycerol backbone in phospholipids. An NMR and X-ray single-crystal study. Biochemistry 27, 9166–9174.

Hesketh, T.R., Smith, G.A., Houslay, M.D., McGill, K.A., Birdsall, N.J.M., Metcalfe, J.C., Warren, G.B., 1976. Annular lipids determine ATPase activity of a calcium-transport protein complexed with dipalmitoyllecithin. Biochemistry 15, 4145–4151.

Hong, M., Schmidt-Rohr, K., Zimmermann, H., 1996. Conformational constraints on the headgroup and *sn*-2 chain of bilayer DMPC from NMR dipolar couplings. Biochemistry 35, 8335–8341.

Horváth, L.I., Drees, M., Beyer, K., Klingenberg, M., Marsh, D., 1990. Lipid–protein interactions in ADP–ATP carrier/egg phosphatidylcholine recombinants studied by spin-label ESR spectroscopy. Biochemistry 29, 10664–10669.

Howard, K.P., Prestegard, J.H., 1995. Membrane and solution conformations of monogalactosyldiacylglycerol using NMR molecular modeling methods. J. Am. Chem. Soc. 117, 5031–5040.

IUPAC-IUB Commission on Biochemical Nomenclature (CBN), 1977. The nomenclature of lipids. Eur. J. Biochem. 79, 11–21.

Iwata, S., Ostermeier, C., Ludwig, B., Michel, H., 1995. Structure at 2.8 Å resolution of cytochrome c oxidase from *Paracoccus denitrificans*. Nature 376, 660–669.

Joo, C.N., Kates, M., 1969. Synthesis of the naturally occurring phytanyl diether analogs of phosphatidyl glycerophosphate and phosphatidyl glycerol. Biochim. Biophys. Acta 176, 278–297.

Jordan, P., Fromme, P., Witt, H.T., Klukas, O., Saenger, W., Krauß, N., 2001. Three-dimensional structure of cyanobacterial photosystem I at 2.5 Å resolution. Nature 411, 909–917.

Jormakka, M., Tornroth, S., Byrne, B., Iwata, S., 2002. Molecular basis of proton motive force generation: structure of formate dehydrogenase-*N*. Science 295, 1863–1868.

Kates, M., Moldoveanu, N., Stewart, L.C., 1993. On the revised structure of the major phospholipid of *Halobacterium salinarum*. Biochim. Biophys. Acta 1169, 46–53.

King, M.D., Marsh, D., 1987. Headgroup and chain length dependence of phospholipid self-assembly studied by spin-label electron spin resonance. Biochemistry 26, 1224–1231.

Kleywegt, G.J., Henrick, K., Dodson, E.J., van Aalten, D.M.F., 2003. Pound-wise but penny-foolish: how well do micromolecules fare in macromolecular refinement? Structure 11, 1051–1059.

Klyne, W., Prelog, V., 1960. Description of steric relationships across single bonds. Experientia 16, 521–523.

Kurisu, G., Zhang, H., Smith, J.L., Cramer, W.A., 2003. Structure of the cytochrome b_{6f} complex of oxygenic photosynthesis: tuning the cavity. Science 302, 1009–1014.

Lange, C., Nett, J.H., Trumpower, B.L., Hunte, C., 2001. Specific roles of protein-phospholipid interactions in the yeast cytochrome bc_1 complex structure. EMBO J. 20, 6591–6600.

Lee, A.G., 2003. Lipid–protein interactions in biological membranes: a structural perspective. Biochim. Biophys. Acta 1612, 1–40.

Li, S., Lin, H.N., Wang, Z.Q., Huang, C., 1994. Identification and characterization of kink motifs in 1-palmitoyl-2-oleoylphosphatidylcholines: a molecular mechanics study. Biophys. J. 66, 2005–2018.

Liu, Z.F., Yan, H.C., Wang, K.B., Kuang, T.Y., Zhang, J.P., Gui, L.L., An, X.M., Chang, W.R., 2004. Crystal structure of spinach major light-harvesting complex at 2.72 Å resolution. Nature 428, 287–292.

Luecke, H., Schobert, B., Richter, H.-T., Cartailler, J.-P., Lanyi, J.K., 1999. Structure of bacteriorhodopsin at 1.55 Å resolution. J. Mol. Biol. 291, 899–911.

Marsh, D., 1974. Statistical mechanics of the fluidity of phospholipid bilayers and membranes. J. Membr. Biol. 18, 145–162.

Marsh, D., 1995. In: Lee, A.G. (Ed.), Biomembranes. JAI Press, Greenwich, CT, pp. 137–186.

Marsh, D., 2003. Lipid-binding proteins: structure of the phospholipid ligands. Protein Sci. 12, 2109–2117.

Marsh, D., Horváth, L.I., 1998. Structure, dynamics and composition of the lipid–protein interface. Perspectives from spin-labelling. Biochim. Biophys. Acta 1376, 267–296.

Marsh, D., Páli, T., in press. Conformation and chain order of lipids in crystals of transmembrane proteins.

McAuley, K.E., Fyfe, P.K., Ridge, J.P., Isaacs, N.W., Cogdell, R.J., Jones, M.R., 1999. Structural details of an interaction between cardiolipin and an integral membrane protein. Proc. Natl. Acad. Sci. U.S.A. 96, 14706–14711.

Meier, P., Sachse, J.-H., Brophy, P.J., Marsh, D., Kothe, G., 1987. Integral membrane proteins significantly decrease the molecular motion in lipid bilayers: a deuteron NMR relaxation study of membranes containing myelin proteolipid apoprotein. Proc. Natl. Acad. Sci. U.S.A. 84, 3704–3708.

Mizushima, T., Yao, M., Inoue, N., Aoyama, H., Yamashita, E., Yamaguchi, H., Tsukihara, T., Nakashima, R., Shinzawa-Itoh, K., Yaono, R., Yoshikawa, S., 1999. Structure of phospholipids in a membrane protein complex, bovine heart cytochrome *c* oxidase. Acta Crystallogr. A55 (Abstr. P06.04.069).

Moser, M., Marsh, D., Meier, P., Wassmer, K.-H., Kothe, G., 1989. Chain configuration and flexibility gradient in phospholipid membranes. Comparison between spin-label electron spin resonance and deuteron nuclear magnetic resonance, and identification of new conformations. Biophys. J. 55, 111–123.

Nogi, T., Fathir, I., Kobayashi, M., Nozawa, T., Miki, K., 2000. Crystal structures of photosynthetic reaction center and high-potential iron–sulfur protein from *Thermochromatium tepidum*: thermostability and electron transfer. Proc. Natl. Acad. Sci. U.S.A. 97, 13561–13566.

Oldfield, E., 1982. In: Martonosi, E.N. (Ed.), Membranes and Transport. Plenum Press, New York, pp. 115–123.

Pascher, I., 1996. The different conformations of the glycerol region of crystalline acylglycerols. Curr. Opin. Struct. Biol. 6, 439–448.

Pascher, I., Sundell, S., 1986. Membrane lipids: preferred conformational states and their interplay. The crystal structure of dilauroylphosphatidyl-*N*,*N*-dimethylethanolamine. Biochim. Biophys. Acta 855, 68–78.

Pascher, I., Lundmark, M., Nyholm, P.-G., Sundell, S., 1992. Crystal structures of membrane lipids. Biochim. Biophys. Acta 1113, 339–373.

Pascher, I., Sundell, S., Harlos, K., Eibl, H., 1987. Conformation and packing properties of membrane lipids: the crystal structure of sodium dimyristoylphosphatidylglycerol. Biochim. Biophys. Acta 896, 77–88.

Pearson, R.H., Pascher, I., 1979. The molecular structure of lecithin dihydrate. Nature (Lond.) 281, 499–501.

Pebay-Peyroula, E., Dahout-Gonzalez, C., Kahn, R., Trézéguet, V., Lauquin, G.J.M., Brandolin, G., 2003. Structure of mitochondrial ADP/ATP carrier in complex with carboxyatractyloside. Nature 426, 39–44.

Pebay-Peyroula, E., Rosenbusch, J.P., 2001. High-resolution structures and dynamics of membrane protein–lipid complexes: a critique. Curr. Opin. Struct. Biol. 11, 427–432.

Plesniak, L.A., Yu, L., Dennis, E.A., 1995. Conformation of micellar phospholipid bound to the active site of phospholipase A_2. Biochemistry 34, 4943–4951.

Ponder, J.W., Richards, F.M., 1987. Tertiary templates for proteins. Use of packing criteria in the enumeration of allowed sequences for different structural classes. J. Mol. Biol. 193, 775–791.

Powell, G.L., Knowles, P.F., Marsh, D., 1985. Association of spin-labelled cardiolipin with dimyristoylphosphatidylcholine-substituted bovine heart cytochrome *c* oxidase. A generalized specificity increase rather than highly specific binding sites. Biochim. Biophys. Acta 816, 191–194.

Powell, G.L., Knowles, P.F., Marsh, D., 1987. Spin label studies on the specificity of interaction of cardiolipin with beef heart cytochrome oxidase. Biochemistry 26, 8138–8145.

Russell, N.J., Harwood, J.L., 1979. Changes in the acyl lipid composition of photosynthetic bacteria grown under photosynthetic and non-photosynthetic conditions. Biochem. J. 181, 339–345.

Ryba, N.J.P., Marsh, D., 1992. Protein rotational diffusion and lipid/protein interactions in recombinants of bovine rhodopsin with saturated diacylphosphatidylcholines of different chain lengths studied by conventional and saturation transfer electron spin resonance. Biochemistry 31, 7511–7518.

Scott, D.L., Sigler, P.B., 1994. Structure and catalytic mechanism of secretory phospholipase A_2. Adv. Protein Chem. 45, 53–88.

Seelig, J., Gally, H.U., 1976. Investigation of phosphatidylethanolamine bilayers by deuterium and phosphorus-31 nuclear magnetic resonance. Biochemistry 15, 5199–5204.

Seelig, J., Gally, H.U., Wohlgemuth, R., 1977. Orientation and flexibility of the choline head group in phosphatidylcholine bilayers. Biochim. Biophys. Acta 467, 109–119.

Seelig, J., Seelig, A., Tamm, L., 1982. In: Jost, P.C., Griffith, O.H. (Eds.), Lipid–Protein Interactions. John Wiley & Sons, New York, pp. 127–148.

Stroebel, D., Choquet, Y., Popot, J.L., Picot, D., 2003. An atypical haem in the cytochrome b_6f complex. Nature 426, 413–418.

Sundaralingam, M., 1972. Molecular structures and conformations of phospholipids and sphingomyelins. Ann. N. Y. Acad. Sci. 195, 324–355.

Svensson-Ek, M., Abramson, J., Larsson, G., Törnroth, S., Brzezinski, P., Iwata, S., 2002. The X-ray crystal structures of wild-type and EQ(I-286) mutant cytochrome *c* oxidases from *Rhodobacter sphaeroides*. J. Mol. Biol. 321, 329–339.

Takeda, K., Matsui, Y., Sato, H., Hino, T., Kanamori, E., Okumura, H., Yamane, T., Kamiya, N., Kouyama, T., 2000. Deposition 1QM8 in the Protein Database.

Thunnissen, M.M.G.M., Ab, E., Kalk, K.H., Drenth, J., Dijkstra, B.W., Kuipers, O.P., Dijkman, R., de Haas, G.H., Verheij, H.M., 1990. X-ray structure of phospholipase A_2 complexed with a substrate derived inhibitor. Nature 347, 689–691.

Träuble, H., 1971. The movement of molecules across lipid membranes: a molecular theory. J. Membr. Biol. 4, 193–208.

Tsukihara, T., Aoyama, H., Yamashita, E., Tomizaki, T., Yamaguchi, H., Shinzawa-Itoh, K., Nakashima, R., Yaono, R., Yoshikawa, S., 1996. The whole structure of the 13-subunit oxidized cytochrome *c* oxidase at 2.8 Å. Science 272, 1136–1144.

Tsukihara, T., Shimokata, K., Katayama, Y., Shimada, H., Muramoto, K., Aoyama, H., Mochizuki, M., Shinzawa-Itoh, K., Yamashita, A., Yao, M., Ishimura, Y., Yoshikawa, S., 2003. The low-spin heme of cytochrome *c* oxidase as the driving element of the proton-pumping process. Proc. Natl. Acad. Sci. U.S.A. 100, 15304–15309.

Valiyaveetil, F.I., Zhou, Y.F., MacKinnon, R., 2002. Lipids in the structure, folding, and function of the KcsA K^+ channel. Biochemistry 41, 10771–10777.

van Tilbeurgh, H., Egloff, M.P., Martinez, C., Rugani, N., Verger, R., Cambillau, C., 1993. Interfacial activation of the lipase–procolipase complex by mixed micelles revealed by X-ray crystallography. Nature 362, 814–820.

Warren, G.B., Toon, P.A., Birdsall, N.J., Lee, A.G., Metcalfe, J.C., 1974. Reconstitution of a calcium pump using defined membrane components. Proc. Natl. Acad. Sci. U.S.A. 71, 622–626.

Watts, A., Marsh, D., Knowles, P.F., 1978. Lipid-substituted cytochrome oxidase: no absolute requirement of cardiolipin for activity. Biochem. Biophys. Res. Commun. 81, 397–402.

Yankovskaya, V., Horsefield, R., Törnröth, S., Luna-Chavez, C., Miyoshi, H., Léger, C., Byrne, B., Cecchini, G., Iwata, S., 2003. Architecture of succinate dehydrogenase and reactive oxygen species generation. Science 299, 700–704.

Zhang, Z., Huang, L., Shulmeister, V.M., Chi, Y.-I., Kim, K.K., Hung, L.-W., Crofts, A.R., Berry, E.A., Kim, S.-H., 1998. Electron transfer by domain movement in cytochrome bc_1. Nature 392, 677–684.